16TH EUROPEAN CONFERENCE ON EARTHQUAKE ENGINEERING THESSALONIKI 18 - 21 JUNE 2018

DISAGGREGATION OF SEQUENCE-BASED SEISMIC HAZARD

Eugenio CHIOCCARELLI,[1] Pasquale CITO,[2] Iunio IERVOLINO[3]

ABSTRACT

Earthquakes are typically clustered in both space and time. The largest magnitude events within each cluster, the mainshocks, are the events considered in the classical probabilistic seismic hazard analysis (PSHA) according to which their occurrence is described by a homogeneous Poisson process. Conversely, the seismic threat due to aftershocks can be quantified via a procedure called aftershock probabilistic seismic hazard analysis (APSHA) that describes aftershocks' occurrence via a nonhomogeneous Poisson process, the rate of which depends on the magnitude of the mainshock.
The so-called sequence-based probabilistic seismic hazard analysis (SPSHA) was recently developed; it consists in a hazard integral that accounts for aftershocks in the classical hypotheses of PSHA. The procedure profits of the fact that the clusters can be seen as single events occurring at the same rate of the mainshocks. SPSHA allows to disaggregate the hazard computation providing, among others, the aftershock contribution to the hazard; i.e., the probability that when a threshold intensity measure is exceeded (at least once) in a cluster, the exceedance is due to an aftershock only. Moreover, the classical magnitude-distance disaggregation distribution, that is the joint magnitude and distance probability density function, conditional to the exceedance of the hazard threshold, can be extended to the case of SPSHA.
In the present study, the formulation of SPSHA and disaggregations are recalled. Then, referring to some specific Italian sites, the results of SPSHA and PSHA are compared and discussed.

Keywords: Sequence-based probabilistic seismic hazard analysis; aftershock; earthquake clusters

1. INTRODUCTION

At the state-of-the-art of most advanced structural engineering codes, design seismic accelerations are derived from probabilistic seismic hazard analysis (PSHA; Cornell, 1968, McGuire, 2004). The latter provides, for a site of interest, the ground motion intensity measure (IM) value that corresponds to a given rate of exceedance. The IM is typically an ordinate of a pseudo-acceleration response spectrum, and structures must be designed to withstand values corresponding to rates that are functions of the desired seismic performance.
Although earthquakes generally occur in time-space clusters, only mainshocks, typically the largest magnitude events within each cluster, are usually considered in the assessment of the seismic threat at long-term time scale. A preliminary procedure, generally known as catalog declustering (e.g., Gardner and Knopoff, 1974), is applied to the considered seismic catalogue to isolate the mainshock of each recorded sequence. This allows using the homogeneous Poisson process (HPP) as the counting process describing mainshocks' occurrence in PSHA.
For short-term risk management purposes during seismic sequences, aftershock probabilistic seismic hazard analysis (APSHA) has been developed (Yeo and Cornell, 2009). APSHA models aftershock occurrence via cluster-specific nonhomogeneous Poisson processes (NHPP), the rate of which depends on the magnitude of the mainshock that has triggered the sequence via the modified Omori law (Utsu, 1961).
Recently, it has been demonstrated that it is possible to combine PSHA and APSHA to include the effect

[1] Assistant professor, Università telematica Pegaso, Naples, Italy, eugenio.chioccarelli@unipegaso.it
[2] Ph.D. candidate, Università di Napoli Federico II, Naples, Italy, pasquale.cito@unina.it
[3] Professor, Università di Napoli Federico II, Naples, Italy, iunio.iervolino@unina.it

of aftershocks in long-term probabilistic seismic hazard analysis, still working with a declustered catalog (Iervolino et al., 2014). The procedure for doing so, named sequence-based probabilistic seismic hazard analysis (SPSHA), profits of the consideration that earthquake sequences, made of mainshocks and following aftershocks, can be seen as events occurring at the same rate of the mainshocks (e.g., Boyd, 2012). In Iervolino et al. (2017), SPSHA was applied to the Italian sites using the same source and propagation models at the basis of the design seismic actions adopted by the Italian building code. The aim of the paper was to compare the results of the hazard assessment via PSHA and SPSHA in terms of national hazard maps. It was shown that (i) increments due to SPSHA with respect to PSHA are in general non-negligible, (ii) they are more significant for comparatively higher seismicity areas and (iii) the average increments on national scale increases with the return period.
Starting from the same framework of Iervolino et al. (2017), this contribution is intended to deepen the differences in disaggregation of the seismic hazard when PSHA or SPSHA are of concern. Thus, the remained part of the paper is structured such that the essentials of PSHA and SPSHA are recalled first; then magnitude and distance disaggregation for SPSHA is formulated. Subsequently, after introducing the considered models for Italy, SPSHA results are presented and compared with the corresponding PSHA counterparts for two Italian sites, selected to be representative of two different topical cases of PSHA disaggregation, and located in medium- and high-seismicity areas. Finally, two idealized cases are considered in order to discuss the influence on disaggregation of the aftershock modeling hypotheses.

2. PROBABILISTIC SEISMIC HAZARD ANALYSIS

The main result of PSHA for a site of interest is the average number of earthquakes in one year (i.e., the rate) causing exceedance of a given IM threshold, say im. The rate of exceedance of im, herein indicated as $\lambda_{im,E}$, is typically obtained via Equation 1.[4]

$$\lambda_{im,E} = \nu_E \cdot \int_{r_{E,min}}^{r_{E,max}} \int_{m_{E,min}}^{m_{E,max}} P\left[IM_E > im \mid x,y\right] \cdot f_{M_E,R_E}\left(x,y\right) \cdot dx \cdot dy \tag{1}$$

In the equation, the subscript (E) indicates that the variables and the obtained rate are referred to classical PSHA; this is to differentiate from SPSHA (to follow). Thus, ν_E is the rate, from a declustered catalog (e.g., Reiter, 1990), of earthquake above a minimum magnitude of interest $\left(m_{E,\min}\right)$ and below the maximum magnitude $\left(m_{E,\max}\right)$ of the considered seismic source. The term $P\left[IM_E > im \mid x,y\right]$, provided by a ground motion prediction equation (GMPE), represents the probability that the intensity threshold is exceeded given an earthquake of magnitude $M_E = x$, from which the site is separated by a distance $R_E = y$, where $R_E \in \left(r_{E,\min}, r_{E,\max}\right)$. The term f_{M_E,R_E} is the joint probability density function (PDF) of mainshock magnitude and distance random variables (RVs). Usually these two RVs, in the case of a single seismic source zone, can be considered stochastically independent and f_{M_E} can be, for example, described by a truncated exponential distribution, derived by the Gutenberg-Richter relationship (Gutenberg and Richter, 1944), while f_{R_E} is obtained on the basis of the source-site geometrical configuration. The integral limits are the magnitudes bounding the Gutenberg-Richter relationship and the distances defining the domain of possible R_E values.

[4] The equation is written considering a single seismic source; in the case of multiple seismic sources, say s in number, the same equation is computed one source at a time and the results summed up: $\lambda_{im,E} = \sum_{i=1}^{s} \lambda_{im,E,i}$.

2.1 PSHA disaggregation

Disaggregation of PSHA (Bazzurro and Cornell, 1999) is a procedure that allows identification of the hazard contribution of each magnitude and distance (or other random variables affecting the hazard). A possible result of disaggregation is the joint probability density function (PDF) of $\{M_E = x, R_E = y\}$ conditional to the exceedance of an IM threshold, $f_{M_E,R_E}\left(x,y \middle| IM_E > im\right)$:

$$f_{M_E,R_E}\left(x,y \middle| IM_E > im\right) = \frac{\nu_E \cdot P\left[IM_E > im \middle| x,y\right] \cdot f_{M_E,R_E}\left(x,y\right)}{\lambda_{im,E}}. \quad (2)$$

Iervolino et al. (2011) discusses, with reference to Italy and to spectral pseudo-acceleration, how and why hazard disaggregation may be dependent on both the return period (T_R) of exceedance of *im* and the vibration period the spectral ordinate refer to. Some of the conclusions of that study will be recalled in the following sections.

3. SEQUENCE-BASED PROBABILISTIC SEISMIC HAZARD ANALYSIS

Similar to PSHA, SPSHA evaluates the annual rate of exceedance of a ground motion intensity measure, λ_{im}. This rate is the average number of seismic sequences (mainshocks and following aftershocks) that in one year cause (at least one) exceedance of im. Under the hypotheses for aftershock hazard of Yeo and Cornell (2009), λ_{im} can be computed via Equation 3, which is a generalization of Equation 1, as shown in Iervolino et al. (2014). (Again the equation is written for a single source.)

$$\lambda_{im} = \\ = \nu_E \cdot \left\{ 1 - \iint_{M_E,R_E} P\left[IM_E \le im \middle| x,y\right] \cdot e^{-E\left[N_{A|x}(0,\Delta T_A)\right] \cdot \iint_{M_A,R_A} P\left[IM_A > im \middle| w,z\right] \cdot f_{M_A,R_A|M_E,R_E}(w,z) \cdot dw \cdot dz} \cdot f_{M_E,R_E}\left(x,y\right) \cdot dx \cdot dy \right\}. \quad (3)$$

The terms: ν_E, $P\left[IM_E \le im \middle| x,y\right] = 1 - P\left[IM_E > im \middle| x,y\right]$, and $f_{M_E,R_E}\left(x,y\right)$ are the same defined in Equation 1, as well as $M_E \in \left(m_{E,min}, m_{E,max}\right)$ and $R_E \in \left(r_{E,min}, r_{E,max}\right)$. The exponential term within the integral refers to aftershocks; it is the probability that, in the cluster generated by the mainshock of features $\{M_E = x, R_E = y\}$, none of the aftershocks cause exceedance of im. This probability depends on $P\left[IM_A > im \middle| w,z\right]$ that is the probability that im is exceeded given an aftershock of magnitude $M_A = w$ and source-to-site distance $R_A = z$.

The term $f_{M_A,R_A|M_E,R_E}$ is the distribution of magnitude and distance of aftershocks, which are conditional on $\{M_E, R_E\}$. This distribution can be written as $f_{M_A,R_A|M_E,R_E} = f_{M_A|M_E} \cdot f_{R_A|M_E,R_E}$, where $f_{M_A|M_E}$ is the PDF of aftershock magnitude and $f_{R_A|M_E,R_E}$ is the distribution of the distance of the site to the aftershocks. The aftershock magnitude is bounded by a minimum magnitude, m_{min}, and the mainshock magnitude; i.e., $M_A \in \left(m_{min}, x\right)$. (Note that m_{min} may coincide with the minimum mainshock magnitude; i.e., $m_{min} \equiv m_{E,min}$).

Given the location of the site, the aftershock distance, $R_A \in \left(r_{A,min}, r_{A,max}\right)$, depends on the magnitude and location of the mainshock (see Iervolino et al., 2014, for details). $E\left[N_{A|x}\left(0,\Delta T_A\right)\right]$ is the expected number of aftershocks, conditional to the mainshock of magnitude $M_E = x$, in the ΔT_A time interval, which is the considered length of the aftershock sequence (assuming that the mainshock occurred at

$t=0$). This number, consistent with APSHA, can be computed as in Equation 4, where $\{a,b,c,p\}$ are the parameters of the modified Omori law.

$$E\left[N_{A|x}\left(0,\Delta T_A\right)\right]=\frac{10^{a+b\cdot(x-m_{\min})}-10^{a}}{p-1}\cdot\left[c^{1-p}-\left(\Delta T_A+c\right)^{1-p}\right] \tag{4}$$

3.1 SPSHA disaggregation

Similarly to the ordinary case, disaggregation of the seismic hazard can be performed also in the case of SPSHA. Equation 5 provides the PDF of mainshock magnitude $\left(M_E=x\right)$ and distance $\left(R_E=y\right)$ given that the ground motion intensity of the mainshock, IM_E, or (at least) the maximum ground motion intensity of the following aftershock sequence $\left(IM_{\cup A}\right)$ is larger than the *im* threshold.

$$f_{M_E,R_E|IM_E>im\cup IM_{\cup A}>im}\left(x,y\right)=$$
$$\frac{\nu_E}{\lambda_{im}}\cdot\left\{1-P\left[IM_E\le im\,|\,x,y\right]\cdot e^{-E\left[N_{A|x}(0,\Delta T_A)\right]\cdot\int_{M_A}\int_{R_A}P\left[IM_A>im|w,z\right]\cdot f_{M_A,R_A|M_E,R_E}(w,z)\cdot dw\cdot dz}\right\}\cdot f_{M_E,R_E}\left(x,y\right) \tag{5}$$

Moreover, it can be useful to quantify the probability that, given the *im* exceedance, such exceedance is caused by an aftershock rather than by a mainshock. This probability, which quantifies the contribution of aftershocks to hazard, is recalled in Equation 6.

$$P\left[IM_E\le im\cap IM_{\cup A}>im\middle|IM_E>im\cup IM_{\cup A}>im\right]=$$
$$\frac{\nu_E}{\lambda_{im}}\cdot\iint_{M_E,R_E}P\left[IM_E\le im\,|\,x,y\right]\cdot\left(1-e^{-E\left[N_{A|x}(0,\Delta T_A)\right]\cdot\iint_{M_A,R_A}P\left[IM_A>im|w,z\right]\cdot f_{M_A,R_A|M_E,R_E}(w,z)\cdot dw\cdot dz}\right)\cdot f_{M_E,R_E}\left(x,y\right)\cdot dx\cdot dy \tag{6}$$

In the equation, $P\left[IM_{\cup A}>im\cap IM_E\le im\middle|IM_{\cup A}>im\cup IM_E>im\right]$ it is the probability that, given that exceedance of *im* has been observed during the mainshock-aftershock sequence, $\left(IM_E>im\cup IM_{\cup A}>im\right)$, it was in fact an aftershock to cause it, while the mainshock was below the threshold: i.e., $\left(IM_{\cup A}>im\cap IM_E\le im\right)$. All the terms of the equation have been already defined discussing Equation 3; see Iervolino et al. (2017) for full derivation.
In the following, SPSHA disaggregation will be discussed for two Italian sites, also comparing to the PSHA counterpart. For the sake of simplicity and readability, the PDF distributions resulting from Equation 2 and Equation 5 will be referred to as *magnitude-distance disaggregations* in both the PSHA and SPSHA case. The probability resulting from Equation 6 will be identified as *aftershock disaggregation*.

4. SOURCE MODELS

Stucchi et al. (2011) describes the models and analyses at the basis of Italian hazard assessment, which is at the basis of the engineering structural seismic actions according to the enforced code in the country. Such analyses are carried out via a logic tree made of several branches. Among them, the branch identified as *921* is the one producing the results claimed to be the closest to those provided by the full logic tree. Therefore, the same models of the branch 921 are adopted in this study for both PSHA and APSHA.

4.1 Mainshock seismic source zones

The seismic source model is the one by Meletti et al. (2008) and it is made of thirty-six areal seismic source zones shown in Figure 1a (this model is common to all the branches of the cited logic tree). The seismicity of each zone is represented by the *activity rates*, that are annual rates of earthquakes occurrence associated to each bin of surface-waves magnitude; the width of the bins, is 0.3. The activity rates were provided by Carlo Meletti (personal communication) and are graphically shown in Figure 1b as a function of the central magnitude value of each bin. As shown, the lowest bin is generally centered on magnitude (*M*) 4.3, but the zone 936, which is the Etna's volcanic area, has a central magnitude of the lowest bin equal to 3.7. The maximum magnitude depends on the zone of interest.

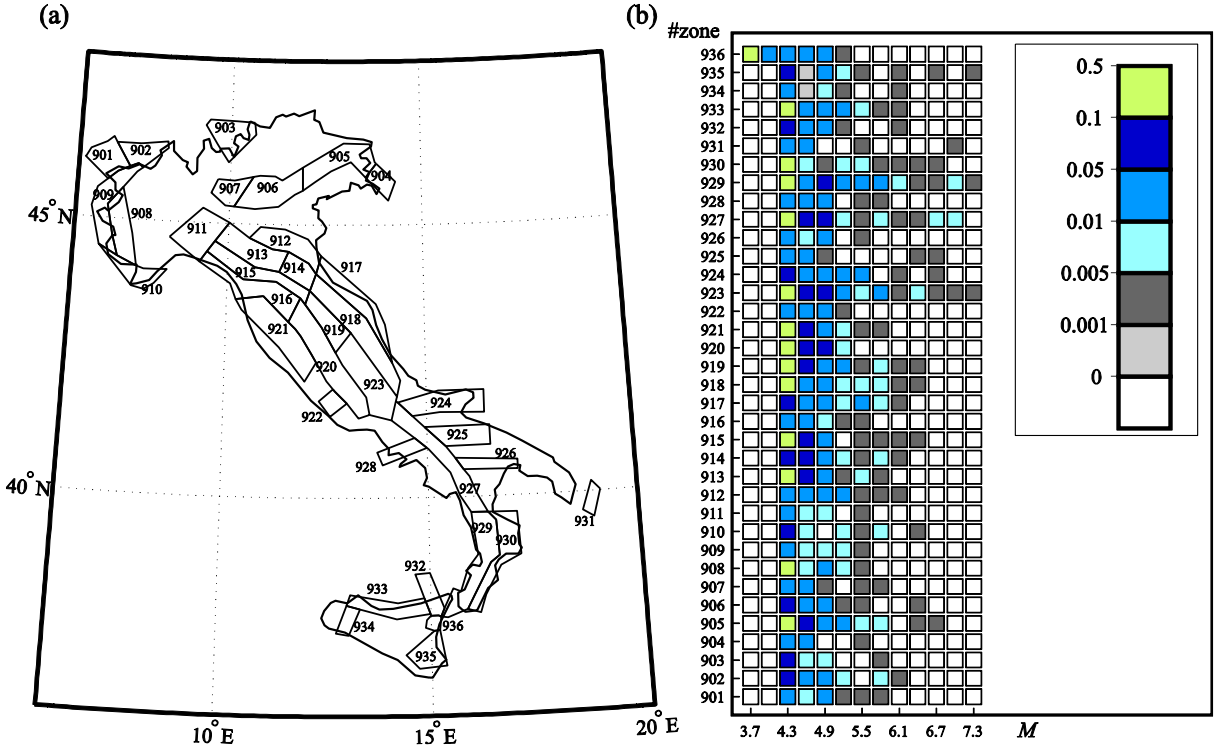

Figure 1. The seismic source zone model for Italy, according to the model of Meletti et al. (2008): (a) geographical distribution of the zones; (b) activity rates values for each bin of magnitude.

4.2 Ground motion prediction equation

Ambraseys et al. (1996) is the adopted GMPE to obtain $P\left[IM_E > im \mid x,y\right]$ (rock soil site class is always assumed herein). The GMPE is applied within its definition ranges of magnitude and distance: these are, surface magnitude between 4.0 and 7.5 and the closest horizontal distance to the surface projection of the fault plane up to 200 km. The effects of earthquakes with magnitude and distance outside these intervals are neglected in the analyses. Assuming a uniform epicenter distribution in each seismogenic zone, epicentral distance is converted into the metric required by the GMPE according to Montaldo et al. (2005). The style-of-faulting correction factors proposed by Bommer at al. (2003) are also applied to the GMPE in accordance with the rupture mechanism associated to each seismic source zone in the model by Meletti et al. (2008).

The Ambraseys et al. (1996) GMPE is also used for $P\left[IM_A > im \mid w,z\right]$ (Equation 3); i.e., it is assumed that the same GMPE is able to describe the ground motion propagation of both mainshock and aftershocks. In the case of aftershocks, the style of faulting is maintained equal to the one used for the mainshock.

4.3 Aftershock models

For SPSHA, the model of Lolli and Gasperini (2003) for generic Italian aftershock sequences is chosen. According to it, the parameter of Equation 4 are $a=-1.66$, $b=0.96$, $c=0.03$ (in days), $p=0.93$. Moreover, it is assumed that the minimum magnitude of generated aftershocks (m_{min}) corresponds to the minimum mainshock magnitude of the seismic source zones $(m_{min} \equiv m_{E,min})$.

Regarding the geographic distribution of aftershocks, it is assumed that they are located, with uniform probability, in a circular area centered on the mainshock location. The size of this area, S_A, depends on the magnitude of the mainshock $(M_E = x)$ via Equation 7, in squared kilometers (Utsu, 1970).

$$S_A = 10^{x-4.1} \tag{7}$$

5. NUMERICAL RESULTS

In Iervolino et al. (2017) the results of SPSHA and the PSHA counterpart are presented in terms of hazard maps on the national scale for fixed return periods and two spectral periods. The cited study focused the attention on the hazard increments when the aftershock effect are considered. It was shown that the absolute hazard increments due to SPSHA with respect to PSHA increase with the return period in average on national scale, while percentage increments have a non-monotonic trend with T_R (depending on the considered site). Here, the attention is focused on the both types of hazard disaggregations presented in Section 3.1 above, with the twofold aim of deepen the trend of aftershock disaggregation as a function of the return period and discuss the differences between magnitude-distance disaggregation distributions in the case of PSHA and SPSHA .

For the intended purposes, two sites are selected: Frosinone in central Italy (13.37°E, 41.64°N) and Messina in southern Italy (15.55°E, 38.19°N). The selection of these two sites is motivated by two reasons. First, they are representative of the medium- (Frosinone) and high-seismicity (Messina) Italian sites. Then, their geographical location with respect to the seismic sources makes the two sites representative of two typical situations in terms of earthquakes most contributing to the hazard. Indeed, Messina is enclosed into zone 929, one of three Italian zones with largest maximum magnitude (see Figure 1b). As a consequence, according to the source model, the site could be hit by very strong events (>M7.3) at zero source-to-site distance. The other seismic zones potentially affecting the hazard of the site may produce weaker (or equal magnitude, in the case of zone 935) and more distant earthquakes. Thus, it can be anticipated that hazard contributions of the other zones are comparatively smaller with respect to the contribution of zone 929 (see also Iervolino et al. 2011). This will result unimodal magnitude-distance disaggregation to follow.

On the other hand, the site of Frosinone is within the zone 920 (maximum magnitude 5.35) and is close to the more seismically active zone 923 (maximum magnitude 7.45). Thus, the zero-distance events for Frosinone are characterized by a maximum magnitude that is much lower than the more distant events generated by the zone 923 (the minimum distance of Frosinone from the boundaries of the zone 923 is about 22 km). This suggests that both zones have significant effects on the hazard of the site and the magnitude-distance disaggregation distributions are, in some cases depending on the return period and on the spectral period being disaggregated, bimodal. Further details are presented in the following section. All calculations of the following sections are carried out via a recent version of the software described in Iervolino et al. (2016).

5.1 Frosinone

Results of hazard assessment for Frosinone are given in Figure 2. More specifically, Figure 2a shows the site location and the twelve seismogenic zones within 200 km (i.e., the definition range of the adopted GMPE). Uniform hazard spectra (UHS') in terms of pseudo-acceleration (Sa) for the four return periods of $50yr$, $475yr$, $975yr$ and $2475yr$ are reported in Figure 2b. The spectra, indicated as PSHA_{Tr} and SPSHA_{Tr}, are computed considering the forty-seven natural vibration (spectral)

periods, T, between zero and two seconds provided by the GMPE. Increments between SPSHA and PSHA for the selected return periods are reported in Figure 2c as a function of the spectral period. Hazard increments are within 7% and 13% for all the vibration periods and the largest values of increments are associated to the lowest return period.

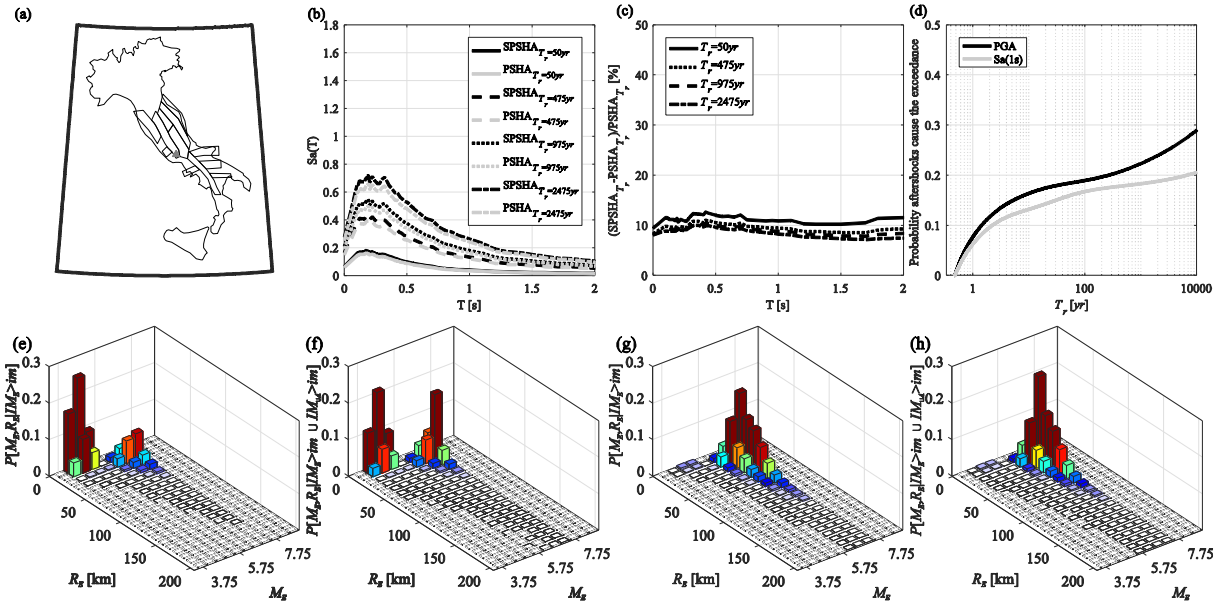

Figure 2. Results of hazard analyses for Frosinone: (a) location of the site and seismic areal zones contributing to its hazard; (b) UHS' for 50yr, 475yr, 975yr and 2475yr; (c) hazard increments as a function of the spectral period and for fixed return periods; (d) aftershock disaggregations for PGA and $Sa(1s)$; (e) and (g) magnitude and distance disaggregation distributions according to PSHA for PGA and $Sa(1s)$ respectively and $T_R = 10000\,yr$; (f) and (h) magnitude and distance disaggregation distributions according to SPSHA for PGA and $Sa(1s)$ respectively and $T_R = 10000\,yr$.

Aftershock disaggregation is reported in Figure 2d as a function of the increasing return period. The considered intensity measures are the peak ground acceleration (PGA) and the pseudo-spectral acceleration at 1 second spectral period $Sa(1s)$. As discussed, aftershock disaggregation according to Equation 6 provides the probability that, once exceedance of *im* is observed, it is caused by an aftershock rather than a mainshock; in this sense, it may help in assessing the contribution of aftershock to hazard. These curves show a monotonic shape: the longer the return period, the higher the probability that aftershocks are causative of the *im* exceedance. Such a trend looks reasonable recalling that increasing the return period (i.e., increasing the *im* threshold), the magnitude of earthquakes most contributing to the hazard tend to increase (see for example Iervolino et al, 2011) and larger magnitude mainshocks generate longer and with larger magnitudes aftershock sequences. However, the trend of Figure 2d is not common to all the Italian sites as demonstrated by the results shown for Messina (see the next section). The reason behind these differences will be explained in Section 5.3.

The second line of panels in Figure 2 is dedicated to the magnitude-distance disaggregation distributions. Such a distributions are reported discretized per bins of magnitude and distance. The dimension of each bin is M0.5 and 10km, respectively (but the first bin of distance is from 0 to 5km). The figures show such disaggregations computed for PGA (Figure 2e and Figure 2f) and $Sa(1s)$ (Figure 2g and Figure 2h). In the panel, Figure 2e and Figure 2g are from Equation 2 while Figure 2f and Figure 2h are from Equation 5.[5] To maximize the possible difference among SPSHA and PSHA disaggregations, the

[5] In the plots, the symbols $f_{M_E,R_E}(x,y|IM_E > im)$ and $f_{M_E,R_E|IM_E>im\cup IM_{\cup A}>im}(x,y)$ are replaced by $P[M_E,R_E|IM_E > im]$ and $P[M_E,R_E|IM_E > im \cup IM_{\cup A} > im]$ respectively because the continuous magnitude

selected return period is 10000 years, which corresponds to the maximum of the aftershock disaggregation, shown in Figure 2d. However, it should be noted that aftershock disaggregation keeps increasing for return periods larger than those considered here and so differences among magnitude-distance disaggregations, although if not shown here for the sake of brevity.

Figure 2e shows two modal bins corresponding to $\{4.5 \le M_E \le 5; 0 \le R_E \le 5\}$ and $\{7.0 \le M_E \le 7.5; 15 \le R_E \le 25\}$. The former is due to the zone 920 while the latter is from zone 923. Comparison among Figure 2e and Figure 2g confirms one of the results of Iervolino et al. (2011): the disaggregation is dependent on the considered spectral period and, in case of bimodal disaggregation distribution, when the spectral period increases, the hazard contribution of stronger and more distant seismic events may increase. The novel result can be derived by the comparison of the PGA disaggregations in Figure 2e (PSHA) and Figure 2f (SPSHA). Although the two distributions are characterized by the same two modal values, it is apparent that when the aftershock effect to the hazard is considered, the modal value associate to higher magnitude-distance events becomes comparatively more significant. This is because clusters generated by higher magnitude events are more likely exceeding the *im* threshold.

On this issue, it can be added that comparison of the magnitude-distance disaggregations of PGA for return periods higher than 10000 years, shows that, in the case of SPSHA, the first modal value become equal to $\{7.0 \le M_E \le 7.5; 15 \le R_E \le 25\}$, while it remains $\{4.5 \le M_E \le 5; 0 \le R_E \le 5\}$ for PSHA. When $Sa(1\text{s})$ is of concern (Figure 2g and Figure 2h), the differences among PSHA and SPSHA are less significant because, as recalled, the stronger and more distant events are the most contributing to hazard even in the PSHA case.

5.2 Messina

The results for the site of Messina are reported in Figure 3. The site is on the boundary of zone 929 and the eight zones reported in Figure 3a are those within the distance definition range of the GMPE. UHS' for the four return periods are shown in Figure 3b. Hazard increments (Figure 3c) due to SPSHA with respect to PSHA are, for this site, between about 12% and 25% for vibration periods up to one second and between 10% and 13 % for higher spectral periods. Hazard disaggregation is reported in Figure 3d. Its trend is completely different with respect to Frosinone. Indeed, aftershock disaggregation increases with the return period until it reaches a maximum equal to 0.32 for PGA and 0.18 for $Sa(1\text{s})$. Then, for both the IMs, it starts decreasing. The return period corresponding to the maximum is 1150 and 1350 years for PGA and $Sa(1\text{s})$, respectively.

Magnitude-distance disaggregation distribution are reported in the same figure for PGA and $Sa(1\text{s})$. Similarly to the previous case, Figure 3e and Figure 3g are computed via Equation 2 while Figure 3f and Figure 3h are from Equation 5. The considered return periods are those for which the aftershock disaggregations of Figure 3d are maximum, that is, 1150 and 1350 years. All the four distributions have a single modal value equal to $\{7.0 \le M_E \le 7.5; 5 \le R_E \le 15\}$ indicating that the earthquakes most contributing to the hazard are from the zone 929. Comparison between PSHA and SPSHA magnitude-distance disaggregation for PGA (Figure 3e and Figure 3f, respectively) shows that considering aftershocks reduce the conditional probabilities of low magnitudes and increases the ones of high magnitude. This is in accordance with what observed for Frosinone, even if applied to the case of unimodal disaggregations. In accordance with what discussed for Frosinone is also the comparison between disaggregations when $Sa(1\text{s})$ is of concern: differences between PSHA and SPSHA are minor.

---

and distance random variables are represented in a discretized form.

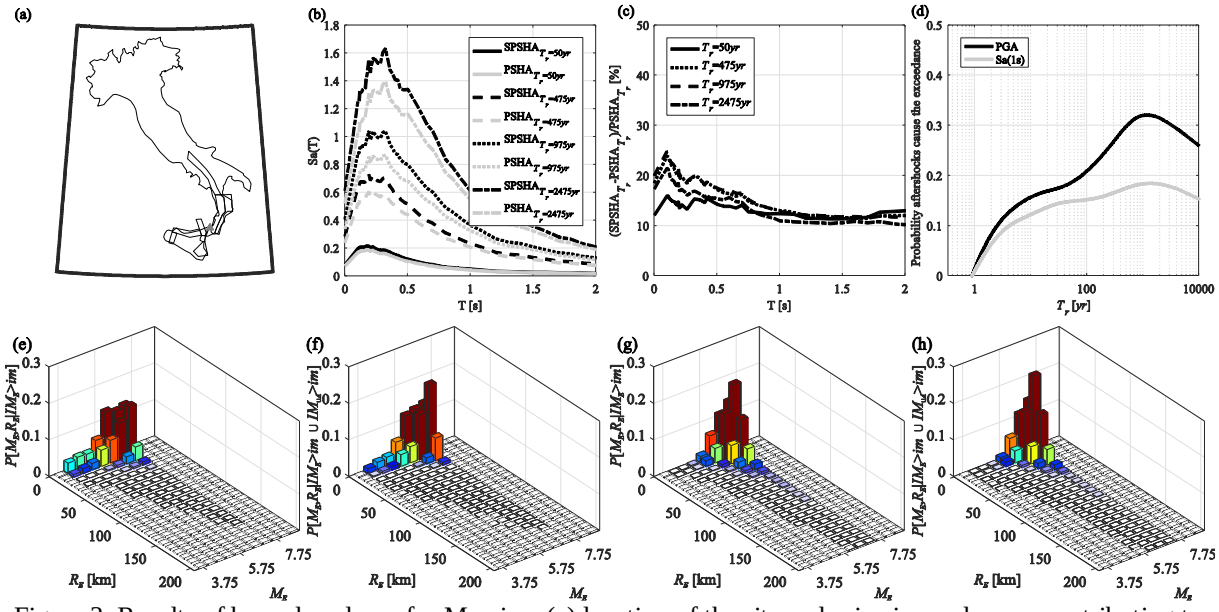

Figure 3. Results of hazard analyses for Messina: (a) location of the site and seismic areal zones contributing to its hazard; (b) UHS' for 50yr, 475yr, 975yr and 2475yr; (c) hazard increments as a function of the spectral period and for fixed return periods; (d) aftershock disaggregations for PGA and $Sa(1s)$; (e) and (f) magnitude and distance disaggregation distributions for PGA and $T_R = 1150yr$ according to PSHA and SPSHA, respectively; (g) and (h) magnitude and distance disaggregation distributions for $Sa(1s)$ and $T_R = 1350yr$ according to PSHA and SPSHA, respectively.

5.3 Source-to-site distance effect on aftershocks disaggregation

The trend of aftershock disaggregation as a function of the increasing return period may be significantly different from site to site (see Figure 2d and Figure 3d). The thesis addressed in this section is that such differences are due to the adopted hypothesis about the spatial distribution of aftershocks around the mainshock. This is discussed considering two simplified scenarios in which the hazard of the site is assumed to be affected by one point-like seismic source producing mainshocks of single magnitude, $M_E = 7.3$. The sole difference between the two scenarios is the relative site-source location. This is chosen in order to be representative of the distance modal value of the magnitude-distance SPSHA disaggregation of the Messina and Frosinone sites, when a high return period is disaggregated. Thus, in the scenarios here analysed, the mainshock source-to-site distance, R_E, equals to zero and twenty kilometers, respectively. It should also be noted that, the constant magnitude here selected is equal to the mean value of the largest bin of magnitude generated by both the zones 923 and 929.

The two scenarios are represented in Figure 4: the site is represented as a triangle in the figure while the point-like seismic source is the red star. Because the GMPE and aftershock distribution models here adopted are the same described above for the case of Italy, the circular geographic area on which aftershocks are uniformly distributed is known via Equation 7 and is equal to about 1600 square kilometers with a radius of about 22km; this area is represented shaded in the figure.

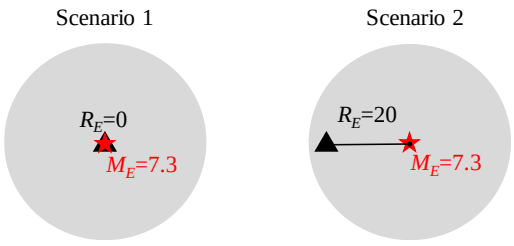

Figure 4. Simplified source-site cases.

For each scenario, the PGA aftershock disaggregation is computed as a function of the return period.

The resulting plots are reported in Figure 5a. When $R_E = 0$, the maximum probability from hazard disaggregation is lower than 0.10 and correspond to a very short return period (about one year). Increasing the return period, aftershock disaggregation monotonically decreases being all the possible aftershocks of lower magnitude and at larger distance than the mainshock. This means that, given that the *im* threshold is exceeded (at least once) during a sequence, the probability that the exceedance is due to an aftershock tends to zero when the *im* threshold (i.e., the return period) increases. This case is, in fact, representative of the aftershocks disaggregations of sites enclosed in seismic source with high seismicity (e.g., the site of Messina).

The opposite trend of aftershock disaggregation is observed in the $R_E = 20$ scenario. In this case, the site is at the boundary of the aftershock geographic distribution thus the distance from the mainshock is (almost) the maximum that allows the occurrence of aftershocks at zero distance. In this condition, with the increasing return period, aftershock disaggregation monotonically increases toward the asymptotic limit of one. This means that the higher is the threshold, the higher the probability that the *im* exceedance during the cluster is due to an aftershock. The results shown in Figure 2d are, in fact, a combination of the two scenarios discussed in this section.

To complete the discussion, an alternative hypothesis on the aftershock geographical distribution is considered: it is assumed that all the aftershocks occur at the mainshock location, $R_A = R_E$. The aftershock disaggregations resulting in these cases are shown in Figure 5b for the same two values of R_E. As apparent, the two plots have a common trend, that is the disaggregation is only slightly influenced by R_E value. This result validates the thesis formulate at the beginning of this section that the observed differences in aftershock disaggregation are due to the hypothesis on the spatial distribution of aftershocks around the mainshock.

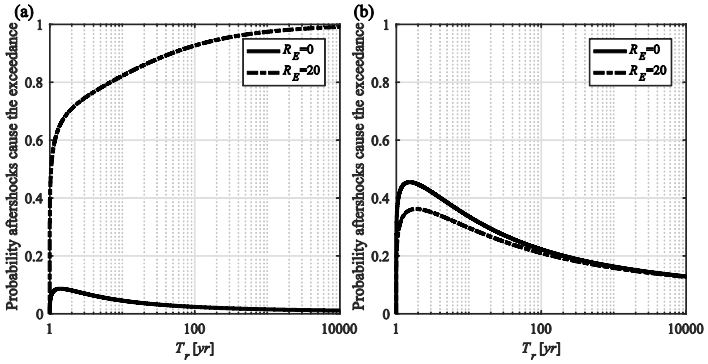

Figure 5. Aftershocks disaggregations for the two seismic scenarios of Figure 6: (a) according to the geographical aftershock distribution of Utsu (1970); (b) assuming all the aftershocks located at the epicenter of the mainshock.

6. CONCLUSIONS

Sequence-based probabilistic seismic hazard analysis (SPSHA) allows to include the aftershocks' effect in probabilistic seismic hazard assessment. The modified hazard integral relies on the modified Omori law and is probabilistically rigorous in the framework of the considered models. The SPSHA stochastic model was introduced in 2014; herein it is applied at two Italian sites in order to discuss effect on hazard disaggregation. The adopted source models are the same lying at the basis of the official seismic hazard of Italy used for structural design. The considered sites are Frosinone and Messina. They are chosen (i) because representative of the medium- and high- seismicity areas in Italy and (ii) because they are representative of two topical conditions characterizing the hazard disaggregations.

For each of the sites, the UHS' with four return periods of exceedance between 50*yr* and 2475*yr* on rock site conditions are shown. Then, the discussion is focused on the comparison between the magnitude and distance disaggregation distributions when SPSHA or PSHA are of concern, and on the trend of aftershock disaggregation with the return period. Regarding the former, it is shown that including the aftershock effect (i.e., in the case of SPSHA) may produce significant effects especially when short

vibration periods are considered. More specifically, disaggregations of SPSHA, with respect to the PSHA counterparts, are characterized by higher probability associated to the high magnitude events. The analyses of aftershock disaggregations show that the trend with return period can be monotonic or non-monotonic depending on the geographical location of the seismic area contributing to the hazard of the site. Finally, it is also demonstrated that this result is strongly influenced by the adopted hypothesis on the symmetrical distribution of aftershock around the mainshock location.

7. ACKNOWLEDGMENTS

This work was developed within the *Rete dei Laboratori Universitari di Ingegneria Sismica* (ReLUIS) 2014-2018 framework programme.

8. REFERENCES

Ambraseys, N. N., K. A. Simpson, and J. J. Bommer (1996). Prediction of horizontal response spectra in Europe, *Earthq. Eng. Struct. D.* **25**, 371-400.

Bazzurro, P. and C. A. Cornell (1999). Disaggregation of seismic hazard. *Bull. Seismol. Soc. Am.* **89**, 501–520.

Bommer, J. J., J. Douglas, and F. O. Strasser (2003). Style-of-faulting in ground-motion prediction equations, *Bull. Earthq. Eng.* **1**, 171–203.

Boyd, O. S. (2012). Including foreshocks and aftershocks in time- independent probabilistic seismic-hazard analyses, *Bull. Seismol. Soc. Am.* **102**, 909-917.

Cornell, C. A. (1968). Engineering Seismic Risk Analysis, *B. Seismol. Soc. Am.* 58, 1583-1606.

Gardner, J. K., and L. Knopoff (1974). Is the sequence of earthquakes in southern California, with aftershocks removed, poissonian?, *Bull. Seismol. Soc. Am*. **60**(5), 1363–1367.

Gutenberg, B. and C. F. Richter (1944). Frequency of earthquakes in California, *B. Seismol. Soc. Am.* 34, 185-188.

Iervolino, I., E. Chioccarelli, and P. Cito (2016). REASSESS V1.0: a computationally-efficient software for probabilistic seismic hazard analysis. Proc. of *VII European Congress on Computational Methods in Applied Sciences and Engineering*, *ECCOMAS*, Crete Island, Greece, 5–10 June.

Iervolino, I., E. Chioccarelli, M. Giorgio (2017). Aftershocks' effects on structural design actions in Italy. *Bull. Seismol. Soc. Am. (in review)*

Iervolino, I., M. Giorgio, and B. Polidoro (2014). Sequence-based probabilistic seismic hazard analysis. *Bull. Seismol. Soc. Am.* **104**, 1006-1012.

Iervolino, I., E. Chioccarelli, and V. Convertito (2011). Engineering design earthquakes from multimodal hazard disaggregation, *Soil Dyn. Earthq. Eng.* **31**(9), 1212–1231.

Lolli, B., and P. Gasperini (2003). Aftershocks hazard in Italy Part I: Estimation of time-magnitude distribution model parameters and computation of probabilities of occurrence, *J. Seismol.* **7**, 235–257.

McGuire, R. K. (2004). Seismic Hazard and Risk Analysis, *Earthquake Engineering Research Institute*, MNO-10, Oakland, California.

Meletti, C., F. Galadini, G. Valensise, M. Stucchi, R. Basili, S. Barba, G. Vannucci, and E. Boschi (2008). A seismic source zone model for the seismic hazard assessment of the Italian territory, *Tectonophysics* **450**, 85–108.

Montaldo, V., E. Faccioli, G. Zonno, A. Akinci, and L. Malagnini (2005). Treatment of ground-motion predictive relationships for the reference seismic hazard map of Italy, *J. Seismol.* **9**, 295–316.

Reiter, L (1990). *Earthquake hazard analysis: issues and insig*hts. Columbia University Press, NY.

Stucchi, M., C. Meletti, V. Montaldo, H. Crowley, G. M. Calvi, and E. Boschi (2011). Seismic hazard assessment (2003–2009) for the Italian building code, *Bull. Seismol. Soc. Am*. **101**, 1885–1911.

Utsu, T. (1970). Aftershocks and earthquake statistics (1): Some parameters which characterize an aftershock sequence and their interrelations. *Journal of the Faculty of Science*, Hokkaido University, *Series 7, Geophysics* **3**, 129-195.

Utsu, T. (1961). A statistical study on the occurrence of aftershocks, *Geophys. Mag.* **30**, 521–605.

Yeo, G. L., and C. A. Cornell (2009). A probabilistic framework for quantification of aftershock ground- motion hazard in California: Methodology and parametric study, *Earthq. Eng. Struct. D.* **38**, 455–60.